Structural and magnetic study of $NdCrTiO_5$ nanoparticles

B Bharati[1,2], P Mohanty[2], ARE Prinsloo[2] and CJ Sheppard[2]

[1]Spectrum Analytical Facility, Faculty of Science, University of Johannesburg, P.O. Box 524, Auckland Park, Johannesburg 2006, South Africa
[2]Cr Research Group, Department of Physics, University of Johannesburg, P.O. Box 524, Auckland Park, Johannesburg 2006, South Africa

E-mail: `bharatib@uj.ac.za`

Abstract. $RCrTiO_5$ compounds shows interesting magnetic behaviour because of the presence of two magnetic sublattices, R^{3+} and Cr^{3+}. $NdCrTiO_5$ is one of the compounds from this group, because only few reports there on $NdCrTiO_5$. Therefore, this contribution focuses on the synthesis, structure, morphology and magnetic properties of nano $NdCrTiO_5$. The orthorhombic crystal structure with lattice parameters, a, b, c is 7.5715 ± 0.0007, 8.7270 ± 0.0008 and 5.7916 ± 0.0006 Å, respectively, was confirmed through x-ray diffraction. The average particle size obtained from the transmission electron microscopy is 33 ± 1 nm, selected area diffraction pattern confirms the crystalline nature of the sample and energy dispersive x-ray spectroscopy confirms the elemental composition. From the temperature-dependent magnetization measurement on the nanoparticles the Néel temperature, temperature, T_N, could not be obtained. This is in contrast with the previously observed T_N in bulk samples at 18 and 21 K and might be due to the reduced size of the material. Further, the ferromagnetic nature of the material was observed from the magnetization as the function of field measurement with coercivity 0.018 ± 0.001 T, 0.019 ± 0.001 T and exchange bias –0.004 ± 0.001 T, –0.003 ± 0.001 T, at 2 K and 10 K, respectively. The observed anomalous properties are discussed considering the size effect.

1. Introduction

In order to improve the device technologies by utilizing various magnetic materials signifying the properties such as, exchange bias (EB), magnetization reversal (MR), spin switching (SS), spin reorientation (SR) and significant magnetocaloric effect (MCE) [1-2]. In a multiferroic material, multiple ferroic states co-exist [1-2] and it is visualized that the co-dependence of the order parameters might contribute to spintronics, in addition to novel memory devices [3-5]. In general, remarkable and exciting physics are probable wherever two or more type of spin sublattices contributes to the observed magnetism in the material [6-8]. RMn_2O_5 (R = rare-earth ions), are the group of compounds, multiferroic in nature, which are attracting the attention of various researchers because of the two contributing magnetic sublattices in the compound [8-10]. These RMn_2O_5 compounds crystallize in an orthorhombic structure, having a space group *Pbam* [8-9]. In these compounds, the sublattice of rare-earth ion is magnetized moderately through the Mn ions [8].

The $RCrTiO_5$ family also has an orthorhombic crystal structure similar to that of RMn_2O_5 [11-12]. In this series of compounds, one can expect to find exceptional and fascinating magnetic behavior because of the co-existence of two magnetic sublattices; Cr^{3+} and R^{3+}. There are only a few reports on these materials until now and most of them are in bulk form [1, 4-7]. Hwang et al. [4] synthesised the $NdCrTiO_5$ and estimated its dielectric constant and pyroelectric current. Das et al. [13], showed magnetic properties such as SR and compensation in bulk $DyCrTiO_5$, as well as in $HoCrTiO_5$ and also observed EB effect. Recently, the reports published on nano $DyCrTiO_5$ and $GdCrTiO_5$, are showing structural and magnetic behavior of the material [14-15]. Exchange coupling among different atoms of an oxide compound having a rare-earth constituent depicts interesting magnetic behavior [1, 4, 13]. A shift in the hysteresis loop across the applied field axis originates in FM-AFM systems because of this exchange coupling. The magnitude of this shifting is known as exchange bias field (H_{ex}) [16]. This exchange bias effect is attributed to the coupling between two magnetic sublattices in the perovskites [17-18]. Zheng et al. [19] also observed an exchange bias effect in $YMnO_3$, which is ascribed to the uncompensated surface spins of the nanoparticles. Nowadays, the world is looking towards the nanostructured materials because of their improved properties, which comes from their enhanced surface-to-volume ratio, as well as uncompensated surface spins [20]. The uncompensated surface spins present significantly modify the magnetic properties as well as other physical properties [20-21]. The change in the structural properties subsequently brings about concomitant changes in the magnetic nature of these materials [22-28].

Nano $NdCrTiO_5$ is one of the promising materials from the RCrTiO$_5$ group yet to be explored. Various magnetic transitions are expected and interpreting the underlying physics responsible for the observed properties of $NdCrTiO_5$ in the nano form will be most interesting. Therefore, this contribution reports on the properties of $NdCrTiO_5$ particles synthesized using the sol-gel technique [20-21], considering x-ray diffraction (XRD), transmission electron microscopy (TEM), magnetization (M) as function of temperature (T) as well as with magnetic field ($\mu_0 H$) results. In addition the modification of magnetic properties on reducing the particle size to nano dimensions will also be discussed in this work.

2. Experimental details

Synthesis of the $NdCrTiO_5$ sample was carried out by the sol-gel method [20-21]. The calculated stoichiometric amounts of $Nd(NO_3)_3$, $Cr(NO_3)_3$ and $Ti(OC_3H_7)_4$ were mixed with ethanol. The solution of the precursors were stirred using a magnetic stirrer [20-21]. Ten milliliters (10 ml) of distilled water was poured into the solution while constantly stirring. The solution was continuously stirred for another half an hour, where after the solution was aged for 24 h. A solid sample was obtained after drying the aged solution and crushed to powder. The powdered sample was then calcined at 800 ºC for three hours in a box furnace. The prepared sample was used for characterization, using x-ray diffraction (XRD) technique with Cu-$K\alpha$ radiation (λ = 1.5406 Å), transmission electron microscope (TEM) and vibrating sample magnetometer (VSM) using a Cryogenic Cryogen Free Physical Properties Measurement System, with a vibrating sample magnetometer insert.

3. Results and discussion

3.1. Structural properties of $NdCrTiO_5$

Firstly, the $NdCrTiO_5$ sample was characterized using XRD techniques to determine the structural properties of the material. The XRD pattern obtained is shown in Figure 1 and it was analyzed using FULLPROF software [29]. The data for the sample shows it having orthorhombic crystal structure with a *Pbam* space group, similarly as was observed in bulk sample prepared by solid state route [4]. The unit cell parameters a, b and c has found to be 7.5715 ± 0.0007, 8.7270 ± 0.0008 and 5.7916 ± 0.0006 Å, respectively, while the cell volume found from the refinement parameters is 382.69 ± 0.06 Å^3. In previous reported data [4] on a polycrystalline bulk $NdCrTiO_5$ sample the cell parameters a, b and c, as 7.5812 ± 0.0002, 8.6803 ± 0.0002 and 5.8123 ± 0.0003 Å, respectively. The XRD patterns could be well resolved with the (hkl) reflections of the orthorhombic structure and the distinct diffraction peaks signify the crystallinity of the particles. No other peaks corresponding to any other impurities have appeared. Minor shifting has been observed in few peak positions because of internal stresses in nano material in line with previously reported results [30]. Along with peak shifting, peak broadening is observed due to nano size of the material (confirmed from the TEM) [31]. In the orthorhombic phase a large number of peaks are observed, but for the sample in the nano form a few peaks are merged [14-15]. In this case the difference between the experimental and calculated data is obtained due to shifting and merging of peaks [30-31]. Further, the crystallite size of the sample has been calculated using Scherrer's formula and found to be 39.0 ± 0.6 nm [14-15].

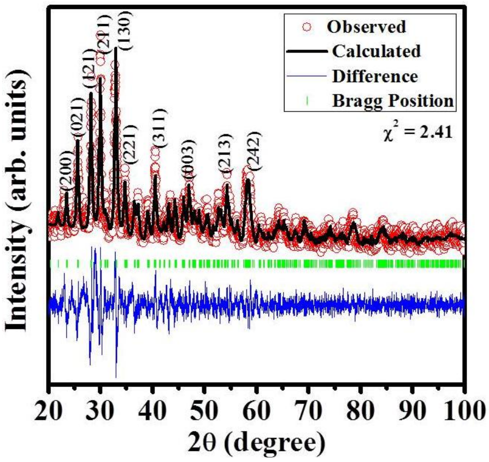

Figure 1. The fitted XRD pattern of the $NdCrTiO_5$ nanoparticles using the FULLPROF program [29].

The TEM image of synthesised $NdCrTiO_5$ is shown in Figure 2(a) and the particle size distribution is shown in Figure 2(b). The sample consist particles of various sizes and shapes. The particle size distribution histogram is fitted using log-normal fit [20]. The average particle size for the synthesized sample is found to be 33 ± 1 nm, with particle size distribution ranging from 20 to 70 nm. Using the sol-gel technique, the $NdCrTiO_5$ nanoparticles are synthesised in a shortened time of only three hours and the calcination temperature is also low compared to solid state synthesis [4]. In the case of bulk $NdCrTiO_5$ the heating time is more than 24 h and temperature is 1300 ºC [4]. Comparing with the earlier synthesis process of $NdCrTiO_5$, the present sol-gel synthesis method is therefore relatively easy and consumes less time. Figure 2(c) shows the TEM image of the selected area electron diffraction (SAED) pattern. From the dotted SAED pattern it is predicted that sample is of crystalline nature [20]. In general, energy-dispersive x-ray spectroscopy (EDS) is used to determine the elements composition, here the EDS is shown in Figure 2(d). The obtained result of elemental composition from EDS is Nd, Cr, Ti, O, C and Cu. The Nd, Cr, Ti and O are from the synthesised material, whereas C and Cu are from the TEM grids. Previous reports [4-5] on bulk $NdCrTiO_5$ samples showed interesting dielectric and magnetoelectric properties. Thus, as a starting point, in the present study the magnetic properties of the nano $NdCrTiO_5$ are investigated.

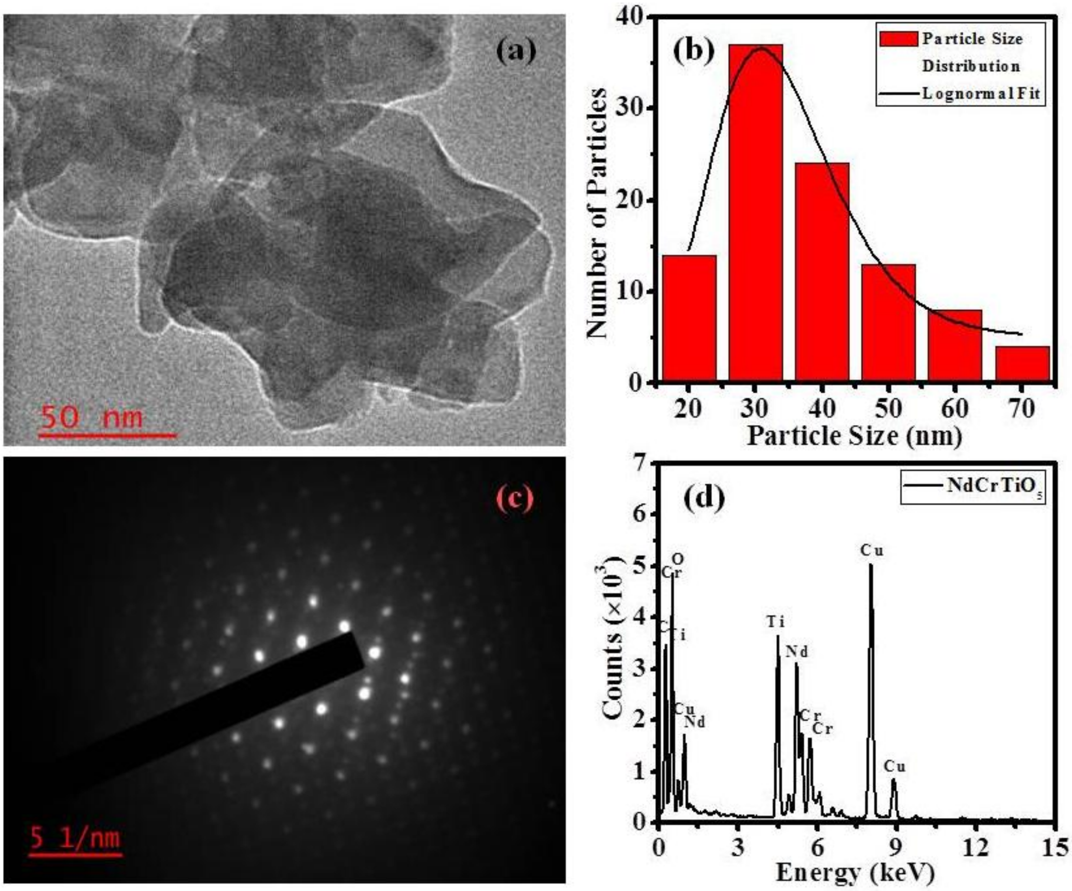

Figure 2. (a) TEM image, (b) particle size distribution using log-normal fit, (c) SAED pattern and (d) energy dispersive x-ray spectroscopy of the $NdCrTiO_5$ nanoparticles.

3.1. Magnetic properties of $NdCrTiO_5$

The dc-magnetization as a function of temperature was carried out for $NdCrTiO_5$ nanoparticles under zero-field-cooling-warming (ZFCW), field-cool-warming (FCW) protocols [14-15]. In ZFCW cycle, the sample is made to cool down to the base temperature of 2 K without any applied magnetic field. Then a magnetic field is applied and magnetization measured from 2 to 300 K. Thereafter, the same applied field is applied and the sample is cooled at the same rate as in ZFCW cycle. After reaching at 2 K, the magnetization (M) as a function of temperature (T) is measured from 2 to 300 K in a FCW measurement [14-15].

The $M(T)$ curves for $NdCrTiO_5$ are shown in Figure 3(a) and (b). Figure 3(a) indicates the measurement carried out at an applied field 0.05 T and Figure 3(b) is for the measurement cycles carried out at applied field 0.1 T. In bulk samples the Néel temperature, T_N, is observed around 18 to 21 K, but this case no such transition is observed in the mentioned temperature range. This might be due to changes in magnetic properties because of nano-sized nature of the material [4-5] studied here. According to literature, it has been found that with changing the size of oxide materials, the various properties can be significantly influenced and changed [21-28]. Based on the previous reports [14-15, 21-28], it can be considered that the change in dimensions can bring about novel properties in the material, as noticed in the present work. As examples, consider earlier reports on bulk $DyCrTiO_5$ [13] indicated SR (spin reorientation), not observed in nanoparticles of the same material [14]. However, in bulk $GdCrTiO_5$ [1] SR is not observed, but in nano $GdCrTiO_5$ [15] SR is observed.

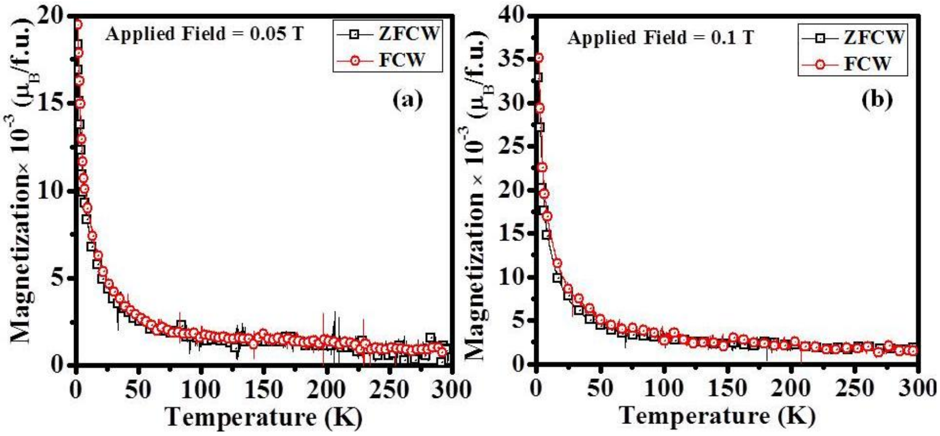

Figure 3. $M(T)$ data for $NdCrTiO_5$ nanoparticles with probing fields of (a) 0.05 T and (b) 0.1 T.

Figure 4 shows the $M(\mu_0 H)$ loops of the $NdCrTiO_5$ nanoparticles, recorded at 2, 10, 30, 60, 80 K with ZFCW protocol. With increase in temperature, the curve indicates paramagnetic behavior of the material. From the curves obtained at 2 and 10 K, the exchange bias (H_{ex}) and coercivity (H_c) is evaluated, using following equations, $H_{ex} = [H_1+H_2]/2$ and for coercivity, $H_c = [H_1-H_2]/2$, where H_1 and H_2 are the positive and negative crossing of the $M(\mu_0 H)$ curves on the applied field axis [17, 32-33]. The obtained value of coercivity, 0.018 ± 0.001, 0.019 ± 0.001 T and exchange bias, –0.004 ± 0.001, –0.003 ± 0.001T, at 2 and 10 K, respectively. The finite values of coercivity indicate the soft ferromagnetic nature of the material [34]. The recorded $M(\mu_0 H)$ curves indicate the weak FM nature of the material.

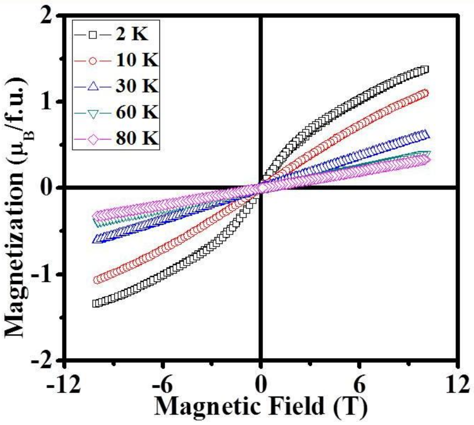

Figure 4. Magnetization as a function of applied field at 2, 10, 30, 60, 80 K, for $NdCrTiO_5$ nanoparticles.

Further, $M(\mu_0 H)$ measurements carried out at 2 K under FCW condition to confirm the exchange bias effect in the material as depicted in Figure 5(a). In Figure 5(b) the zoomed view of the measured curves of both ZFCW and FCW are asymmetric in nature with shifting of hysteresis loop. The ZFCW showing positive exchange bias, whereas FCW condition gives negative exchange bias, that is clearly demonstrate the exchange bias effect of the synthesized sample. Deepak et al. [17], demonstrates that the EB obtained in the single phase, $La_{0.5}Pr_{0.5}CrO_3$, is because of the exchange coupling between Pr^{3+} and Cr^{3+}. EB have been observed in $SmCrO_3$ due to the interaction between Sm^{3+} moment and Cr^{3+} moment [32]. Similarly, $TmCrO_3$ exhibiting EB effect, which obtained due to the interaction of Tm^{3+} and Cr^{3+} [35]. In one of the earlier report, Hong et al. [36] showing EB in a single-phase $NdMnO_3$

system due to the coupling between Nd^{3+} and Mn^{3+}. EB was for the first time observed in $YMnO_3$ nanoparticles, which is attributed to the exchange coupling between uncompensated spins found on the surface of the nanoparticles [19]. In a recently reported nano $DyCrTiO_5$ system EB is ascribed to complex magnetic interaction of surface uncompensated spins between each other [14]. Similar to the reported results, in the present case EB is attributed to the surface uncompensated spins and their magnetic interaction.

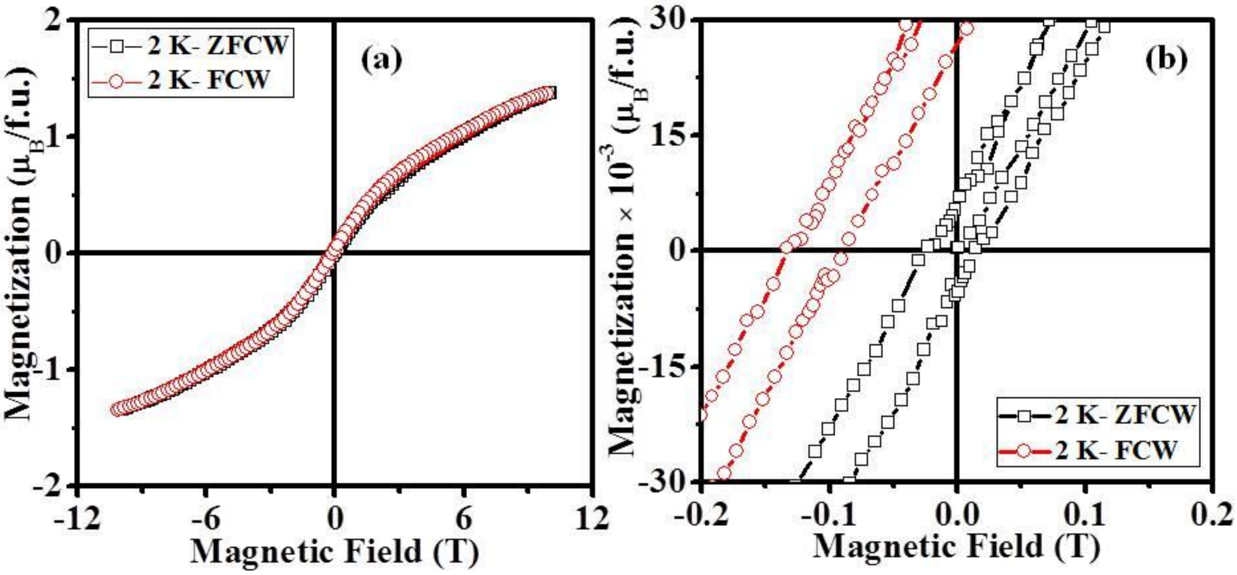

Figure 5. Magnetization as a function of applied field for the $NdCrTiO_5$ nanoparticles (a) at 2 K ZFCW and FCW, (b) zoomed view of the loops.

4. Conclusions

In the present case, $NdCrTiO_5$ nanoparticles were synthesized using a simple sol-gel technique to explore the role of size on structural and magnetic properties. The synthesised $NdCrTiO_5$ nanoparticles were calcined at 800 °C for three hours. The orthorhombic crystal structure was confirmed from the XRD pattern having lattice parameters, a, b, c of 7.5715 ± 0.0007, 8.7270 ± 0.0008 and 5.7916 ± 0.0006 Å, respectively. The nanosize (33 ± 1 nm) of the particles as well as elemental composition of the material was confirmed from the TEM results. Due to nanosize of the material T_N is not observed from the temperature-dependent magnetization measurement, which was observed in bulk samples. Field dependent magnetization study showed the exchange bias effect which is consequence of uncompensated spins on the surface of the material. These observed anomalous properties might be due to the size effect.

Acknowledgments:

Financial aid from the SANRF (Grant No. 120856), as well as the University of Johannesburg (UJ) URC and FRC (Grant Nos. 282810, 083135) is acknowledged. The use of the NEP Cryogenic Physical Properties Measurement System at UJ, obtained with the financial support from the SANRF (Grant No. 88080) and UJ, RSA, is acknowledged. The use of the Spectrum facility in the FoS at UJ is acknowledged.

References

[1] Das M, Roy S, Khan N and Mandal P 2018 *Phys. Rev.* B **98** 104420

[2] Perzanowski M, Zarzycki A, Gregor-Pawlowski J and, Marszalek M 2020 *ACS Appl. Mater. Interfaces* **12** 39926

[3] Blachowicz T and Ehrmann A 2021 *Coatings* **11** 122

[4] Hwang J, Choi ES, Zhou HD, Lu J and Schlottmann P 2012 *Phys. Rev.* B. **85** 024415

[5] Saha J, Sharma G and Patnaik S 2014 *J. Magn. Magn. Mater.* **360** 34

[6] Basu T, Adroja DT, Kolb F, von Nidda HA, Ruff A, Hemmida M, Hillier AD, Telling M, Sampathkumaran EV, Loidl A and Krohns S 2017 *Phys. Rev.* B **96** 184431

[7] Guedes EB, Martins HP, Abbate M, Masunaga SH, Ramirez FE, Jardim RF and Mossanek RJ 2017 *J. Alloy and Compounds* **724** 67

[8] Noda Y, Kimura H, Fukunaga M, Kobayashi S, Kagomiya I and Kohn K 2008 *J. Phys.: Condens. Matter.* **20** 434206

[9] Blake GR, Chapon LC, Radaelli PG, Park S, Hur N, Cheong SW and Rodriguez-Carvajal 2005 *Phys. Rev.* B. **71** 214402

[10] Balli M, Mansouri S, Jandl S, Fournier P and Dimitrov DZ 2017 *Magnetochemistry* **3** 36

[11] Basu T, Singh K, Gohil S, Ghosh S and Sampathkumaran EV 2015 *J. Appl. Phys.* **118** 234103

[12] Greenblatt M, Hornreich RM and Sharon B 1974 *J Solid State Chemistry* **10** 371

[13] Das M, Roy S, Mahalingam K, Ganesan V and Mandal P 2019 *J. Phys.: Condens. Matter.* **32** 035802

[14] Bharati B, Mohanty P, Sheppard CJ and Prinsloo AR 2022 *J. Magn. Magn. Mater.* **546** 168862.

[15] Bharati B, Mohanty P, Sheppard CJ and Prinsloo AR 2022 *AIP Advances* **12** 035245

[16] Morales R, Basaran AC, Villegas JE, Navas D, Soriano N, Mora B, Redondo C, Batlle X and Schuller IK 2015 *Phys. Rev. Lett.* **114** 097202

[17] Deepak, Kumar A and Yusuf SM 2020 *J. Appl. Phys.* **127** 213903

[18] Tang YK, Sun Y and Cheng ZH 2006 *Phys. Rev.* B **73** 174419

[19] Zheng HW, Liu YF, Zhang WY, Liu SJ, Zhang HR and Wang KF 2010 *J. Appl. Phys.* **107** 053901

[20] Bharati B, Sonkar AK, Singh N, Dash D and Rath C 2017 *Mater. Res. Express* **4** 085503

[21] Bharati B, Mishra NC, Sinha AS and Rath C 2020 *Mater. Res. Bulletin* **123** 110710

[22] Bharati B, Mishra NC, Kanjilal D and Rath C 2018 *Applied Surface Science* **428** 723

[23] Bharati B, Mishra NC and Rath C 2018 *Applied Surface Science* **455** 717

[24] Mohanty P, Singh VP, Mishra NC, Ojha S, Kanjilal D and Rath C 2014 *J. Phys. D: Appl. Phys.* **47** 315001

[25] Bharati B and Rath C 2021 *AIP Advances* **11** 035110

[26] Mohanty P, Kabiraj D, Mandal RK, Kulriya PK, Sinha AS and Rath C 2014 *J. Magn. Magn. Mater.* **355** 240

[27] Bharati B and Rath C 2018 *AIP Conference Proceedings* **1942** 050134

[28] Bharati B and Rath C 2020 *AIP Conference Proceedings* **2265** 030336

[29] Rodríguez-Carvajal J 1993 *Physica B: Condensed Matter.* **192** 55

[30] Sen S, Halder SK and Gupta SS 1973 *J. Phys. D: Appl. Phys.***6** 1978

[31] Kumar L, Kumar P, Narayan A and Kar M 2013 *International Nano Letters* **83** 8

[32] Huang S, Zerihun G, Tian Z, Yuan S, Gong G, Yin C and Wang L 2014 *Ceramics International* **40** 13937

[33] Wang L, Rao GH, Zhang X, Zhang LL, Wang SW and Yao QR 2016 *Ceramics International* **42** 10171

[34] Miao XF, Mitsui Y, Dugulan AI, Caron L, Thang NV, Manuel P, Koyama K, Takahashi K, Van Dijk NH, Brück E. Kinetic-arrest-induced phase coexistence and metastability in (Mn, Fe) 2 (P, Si). Physical Review B. 2016 Sep 22;94(9):094426.

[35] Lakhani A, Dash S, Banerjee A, Chaddah P, Chen X and Ramanujan RV 2011 *Applied Physics Letters* Dec 12;99(24):242503.

[36] Hong F, Cheng Z, Wang J, Wang X and S. Dou 2012 *Appl. Phys. Letter* **101** 102411